社団法人 電子情報通信学会
THE INSTITUTE OF ELECTRONICS,
INFORMATION AND COMMUNICATION ENGINEERS

信学技報
TECHNICAL REPORT OF IEICE.

Analysis of Ranging Accuracy for UWB Localization

Marzieh DASHTI†, Mir GHORAISHI†, Katsuyuki HANEDA††, Jun-ichi TAKADA†, and Ken-ichi TAKIZAWA†††

† Graduate School of Engineering, Tokyo Institute of Technology
2-12-1 O-okayama, Meguro-ku, Tokyo, 152-8550 Japan
†† Helsinki University of Technology, Radio Laboratory, FIN-02015 HUT, Finland
††† National Institute of Information and Communications Technology, Kanagawa 239 0847, Japan
E-mail: †{dashti,mir,takada}@ap.ide.titech.ac.jp, ††katsuyuki.haneda@tkk.fi, †††takizawa@nict.go.jp

Abstract In time-of-arrival (ToA) based UWB localization, the accuracy of ranging is presumed. Especially for line-of-sight (LoS) scenarios it is assumed that by estimating the delay for the first-arrival path (assumed to be the LoS) the distance between the transmitter and receiver node can be derived. Using measurement data, we analyze the accuracy of the ranging based on the strongest path and the first-arrival path, the latter of which is dependent on its detection technique. Moreover the influence of frequency bands and signal bandwidth on ranging accuracy is analyzed. This is performed for two allocated mandatory subbands for ranging according to IEEE802.15.4a2007.
Key words Localization, Ranging, UWB

1. Introduction

Ultra-wide-band (UWB) signals are defined as signals with either an absolute bandwidth larger than 500 MHz or a relative bandwidth larger than 20%. This large bandwidth leads to new possibilities for both UWB radars and UWB communications applications from which UWB systems gain interest of researchers [1]. Emerging application of UWB are foreseen for sensor networks as well. Such networks combine low to medium rate communications with positioning capabilities. UWB signaling is specially suitable in this context because it allows centimeter accuracy in ranging. These new possibilities have also been recognized by IEEE, which has been set up a new standardization group 802.15.4a for the creation of a new physical layer for the low data rate communications combined with positioning capabilities; UWB technology is a leading candidate for this standard [2]. Localization based on ToA of radio signals has been an important issue for wideband mobile communication systems and fast developing UWB technologies [3]. In spite of major recent research, precise indoor localization still remains as a challenge facing the research community. The core of this challenge is to understand the cause of large ranging errors in estimating the ToA of the first-arrival path (FAP) between the transmitter (Tx) and the receiver (Rx). Behavior of the ranging error, which we refer to as the ranging error, its relation to the distance between the Tx and the Rx and the bandwidth of the system is needed for development of localization algorithms for precise indoor localization. UWB measurements provide the widest bandwidth and consequently the most accurate measurements of the behavior of the FAP [4]〜[6]. For a precise investigation of the ranging error, we collected a database of UWB channel impulse response measurements at 3.1-10.6 GHz in an office testbed room developed by the National Institute of Information and Communications Technology (NICT) in Japan for measurement proposes. Results of wideband measurement reveal that large ranging errors are caused by severe multipath conditions and frequent occurrence of undetected direct path situations [7]. These results reflect the sensitivity to bandwidth and show that by increasing the bandwidth, ranging error decreases. This paper is further divided into 4 sections: brief description of the measurement data used in this research, description of the proposed scheme for detection of FAP, investigation of the effect of frequency band and frequency bandwidth on ranging accuracy, and finally conclusion.

2. Measurement

The measurements were conducted in an office room and covers wide areas inside it. We planned to measure the channel transfer function of various locations in the room. There were several desks, chairs, and television displays as shown in Figure 1. Walls were made of metal, and the ceiling was composed of plaster board. The floor plan of the room is depicted in Figure 2. Rx antenna was fixed at the corner of the room, whereas the Tx antenna could be positioned

Figure 1 The view of the measurement environment

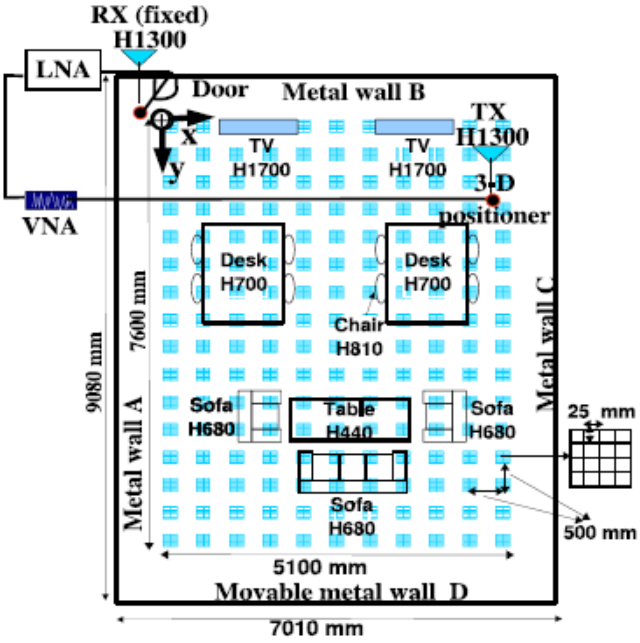

Figure 2 Layout of the measurement environment

at almost any place in the room by the aid of a large spatial scanner covering the whole areas of the room. A small 5×5 array was formed on the horizontal plane to probe the small-scale effects of channels, which is simply referred to as an array; while the array measurement was performed in 168 positions in the room to capture large-scale effects. In total, 4200 spatial samples were measured on the Tx side. Inter-array distance was 0.5 m, and inter-element spacing in the array was 0.25 m. The channel transfer function of a single Tx-Rx combination was measured by a vector network analyzer (VNA). Measurement specifications are summarized in Table 1. The maximum detectable ToA is 200 ns that is the inverse of frequency sampling rate. This was sufficient to capture dominant propagation paths. Line-of-sight (LoS) existed was assured in most Tx positions except for two array positions where the LoS was obstructed by TV sets. The whole measurement took about 6 hours, but there was no moving object during the measurement so that the time-invariance of the angular-delay channel characteristics was ensured. Phase drift of the VNA was carefully compensated during the measurement by performing an internal calibration procedure of the VNA once in two hours.

Since our measurement data and all the analysis in this study were done in allocated subbands in IEEE 802.15.4a standard, we briefly describe the specification of this standard. The IEEE802.15.4a standard defines several frequency bands for the realization of piconets as summarized in Table 39i-UWB PHY band allocation [8]. The band plan defines three band groups: sub-gigahertz, low, and high bands. We will not consider sub-gigahertz band, since the measurement data do not cover that frequency. In the low and high bands, there are mandatory bands where the ranging operation should be assured most (channels 3 and 9), and others are optional. bandwidth of each mandatory channel is 499.2 MHz with various center frequencies. There are also optional channels with larger bandwidth (channels 4, 7, 11 and 15) with bandwidth of 1331.2 MHz. Evaluation of ranging accuracy were assessed in channel 3, 4, 9 and 11. Table 2 shows the specification of these channels.

Table 1 Specification of the measurement

Bandwidth	3.1-10.6 GHz
Measurement equipment	Vector network analyzer Room-wide spatial scanner Low-noise amplifier (30 dB)
Frequency sweeping points	1501
Antenna	UWB monopole
Transmitted power	-17 dBm (CW)
Measured area	5.1×7.6 m^2
Tx-Rx antenna separation	0.6 to 9.3 m
Tx and Rx antenna height	1.3 m above the floor

3. Ranging Error

In ToA-based positioning systems, ToA of FAP is an estimate rather than the ToA of the strongest path (SP). The measured distance between the Tx and Rx antennas are obtained from:

$$d_m = \tau_m \times c \tag{1}$$

where τ_m is the propagation delay of FAP and c is the speed of light. The ranging error e_m then obtained from:

$$e_m = d_m - d \tag{2}$$

where d is the real distance between Tx and Rx antennas. In practice, e_m is a function of the accuracy of measurement of FAP which is a function of the bandwidth of the

Table 2 Band allocation defined in IEEE802.15.4a standard

Channel	f_c (MHz)	Bandwidth(MHz)	Mandatory/Optional
3	4492.8	499.2	Mandatory
4	3993.6	1331.2	Optional
9	7987.2	499.2	Mandatory
11	7987.2	1331.2	Optional

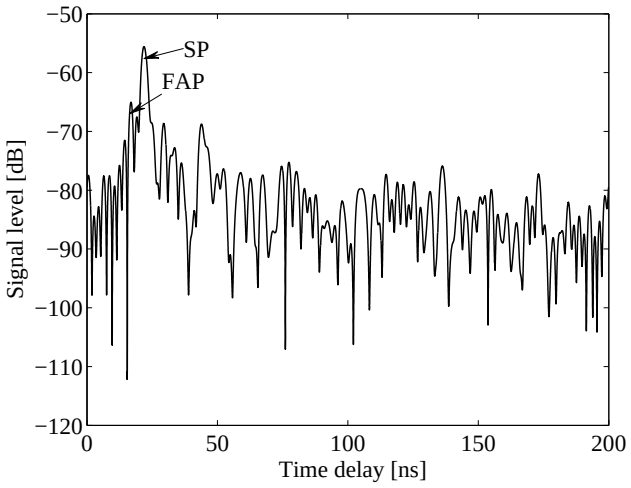

Figure 3 Channel impulse response for an arbitrary position in channel 9

measurement system. Figure 3 illustrated a typical measured channel impulse response in an arbitrary location in the measurement room. It is observed that FAP is not identical to SP in this case. For precise ranging, ToA of FAP shall be used. In the next section we proposed an iterative algorithm for detection of FAP.

4. First Arrival Path Detection Algorithm

Several scheme have been proposed for first arrival detection [9]. We propose an iterative algorithm to calculate the noise floor (NF) to be used in the detection of FAP.

In ToA-based localization systems, ToA of FAP is used for ranging estimate. We expect to obtain the real distance using ToA of FAP. However in some the first-detected path (FDP) is not FAP. In the following the ranging error caused by errornous detected of FAP is discussed.

The algorithm detects the SP, in the first iteration, and then calculates the NF by averaging over the interval $[0, (\tau_{sp} - t_c)]$, where t_c is delay resolution. The interval is $t_c = 0ns$ less than the SP delay to exclude the effect of SP signal and to remove the effect of side lobes. In next iterations this process is repeated for new time interval $[0, (\tau_i - t_c)]$, and it will continue to find the new peak value and the new NF. Here τ_i is ToA of the peak detected in the ith iteration. The algorithm will be continue until finding the first peak higher than the NF by predefined threshold value (L_{th}), which is dependent on bandwidth. Figure 4 shows the flowchart of the proposed iterative algorithm. P_i and NF_i in the flowchart are peak value and NF in the ith iteration. Obviously the value of NF is erroneous in the first iteration but it will give the real NF and FDP after enough iterations.

L_{th} level which the algorithm used for detecting of FAP is chosen different for each channel. To obtain the optimum L_{th} which gives lowest error, we calculated the ranging error using several L_{th}, such as 5, 10,15 and 20 dB. Concerning

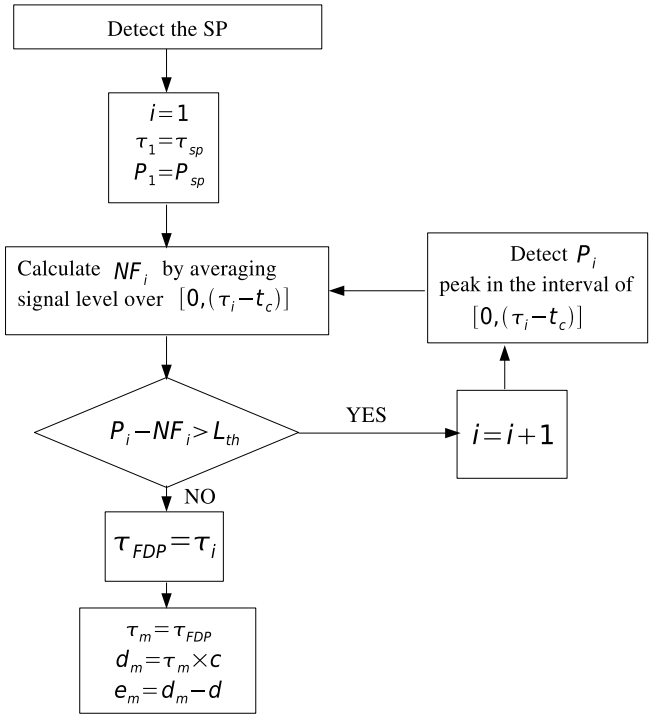

Figure 4 Flowchart of first-arrival path detection algorithm

the difference of SP signal level in different subbands (as shown in Figure 7), these optimum L_{th} value are different for channels with different bandwidth. Table 4 also shows the average μ_e and variance σ_e of ranging error using different L_{th} in different subbands. Figure 5 shows CDF of ranging error using different L_{th} for Channel 4. From the result of ranging analysis in Table 4 and concerning the CDF of ranging error shown in Figure 5,L_{th} was chosen 15 dB for Channel4. Same analysis were done for the other subbands, however we hesitate to show CDF of all of them for the sake of conciseness. For higher bandwidth the algorithm search for the first peak above 15dB from NF, L_{th} is chosen 10dB for channels with lower bandwidth.

Figure 6 shows CDF of calculated NF for Channels 3,4,9 and 11. It is observed that the NF decreases for higher bands and also decrease by increasing the bandwidth. Figure 7 shows CDF of SP signal level for these channels. The peak value decrease in higher bands and also decrease by increasing the bandwidth. Since path loss increase as the frequency increase.

This algorithm has the advantage of obtaining the result

Table 3 σ_e and μ_e of ranging error using different (L_{th}) for different subbands

Channel	5 dB		10 dB		15 dB		20 dB	
	μ_e	σ_e	μ_e	σ_e	μ_e	σ_e	μ_e	σ_e
3	-4.27	4.90	-0.26	7.93	0.83	6.91	1.93	9.09
4	-4.83	4.41	-1.42	3.51	-.0.01	2.90	1.70	4.61
9	-4.16	5.08	-0.22	3.12	1.07	1.66	1.94	1.60
11	-5.05	4.24	-1.05	2.35	0.33	2.08	0.14	2.46

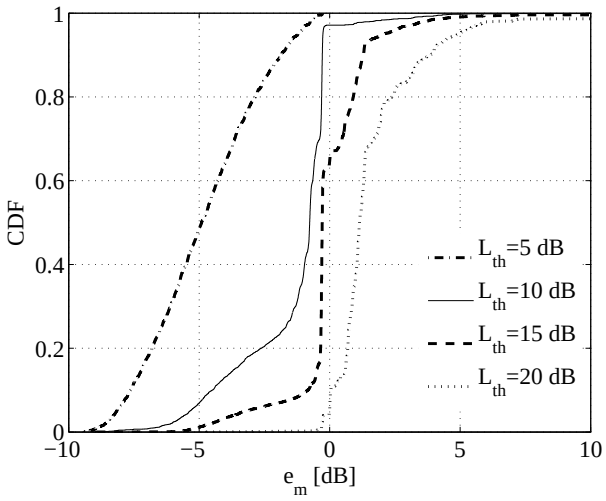

Figure 5 CDF of ranging error using different (L_{th}) for Channel 4

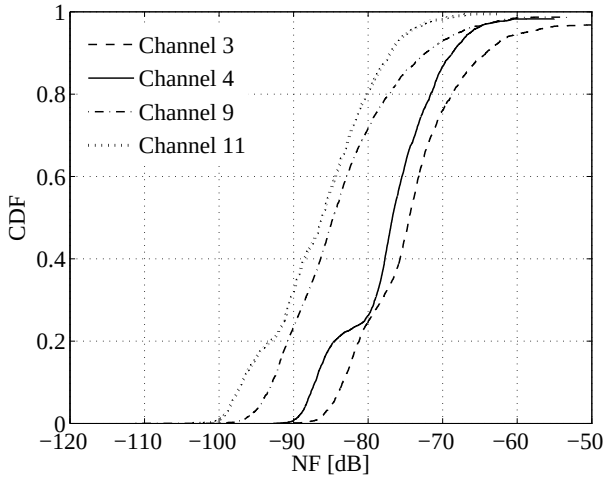

Figure 6 CDF of NF in different subbands

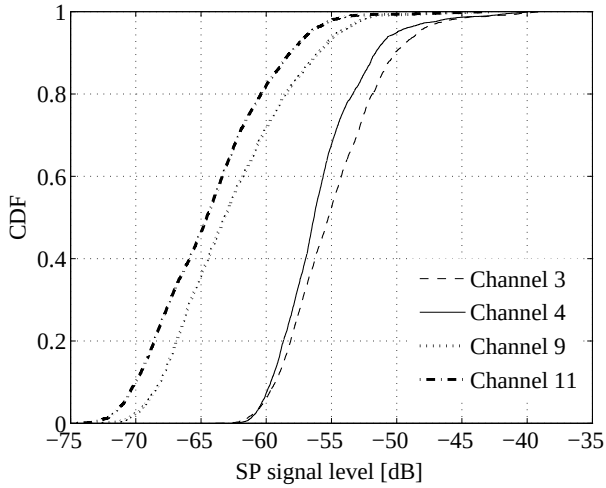

Figure 7 CDF of SP signal level in different subbands

after a few number of iterations for the far points. Also for the close points (Tx and Rx close together) in the lower frequency bands, the averaging over longer intervals in the first

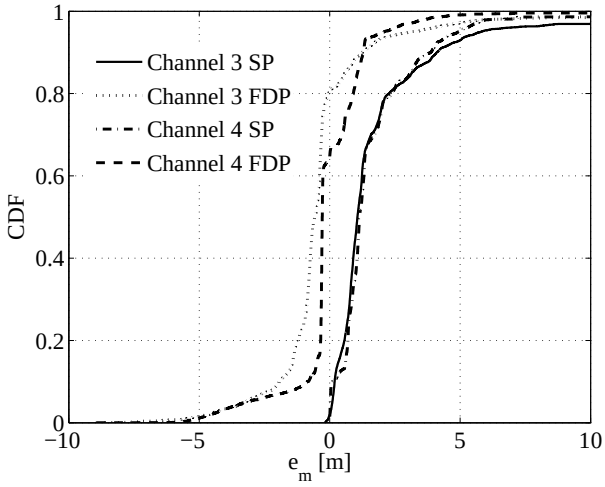

Figure 8 CDF of ranging error by estimation of ToA of SP and FDP in low subbands

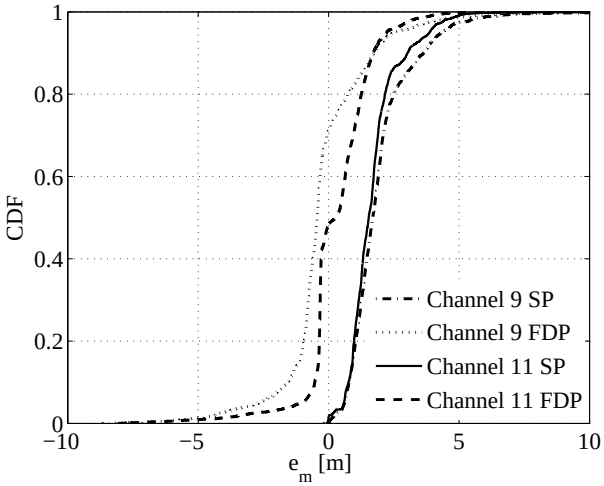

Figure 9 CDF of ranging error by estimation of ToA of SP and FDP, in high subbands

iteration seems to be reliable by using this algorithm.

Evaluation of ranging accuracy were assessed in channels 3,4,9 and 11. The results of this analysis are shown in Table (4). The average and variance of e_m decrease by using FDP instead of SP. The CDF of the ranging errors obtained from using SP and those for FDP derived by algorithm in low subbands and high subbands are exhibited in Figure 8 and 9 respectively. The result shows the algorithm works well for almost all of the positions, however in some cases FAP and FDP are different which causes ranging error. We categorize

Table 4 Variance and average of the ranging error ,by estimation of ToA of SP and FDP, in different subbands

Channel	SP		FDP	
	μ_e	σ_e	μ_e	σ_e
3	1.93	9.08	-0.26	7.93
4	1.73	4.50	-0.01	2.90
9	1.94	1.60	-0.22	3.12
11	1.70	1.20	0.33	2.08

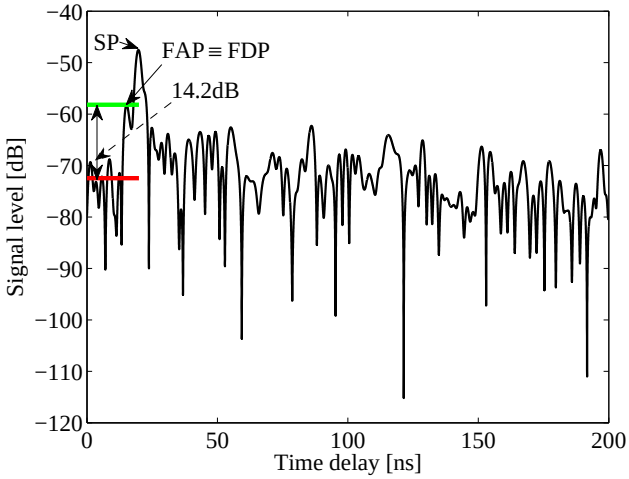

Figure 10 Channel impulse response for an arbitrary position in channel 3

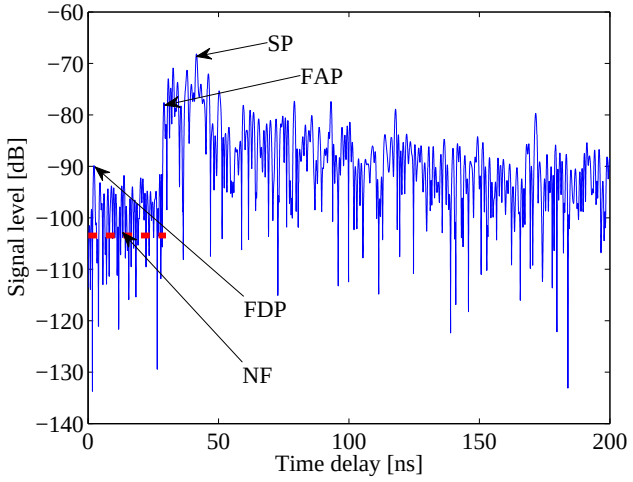

Figure 11 Channel impulse response for an arbitrary position in channel 9

the ranging errors to three main categories; relatively small errors, large positive and large negative errors. Discussion on each of them with an example is given in this section.

Figure 10 shows impulse response of an arbitrary position in the roomin channel 3. By applying the mentioned iterative algorithm, after only 2 iteration, we detect the correct FAP, as shown in Figure 10. The ranging error for this position is 0.2 m, which is a relatively small error where the real distance between Tx and Rx is 4.6 m. However the required ranging accuracy is depended on the application. The calculated NF for this position is -72 dB. The power level of FDP is 14.2 dB more than the calculated NF.

Figure 10 and Figure 3 show the typical impulse responses, which give relatively small minus/positive error respectively. As shown in those figures the peak of channel response gets a little shifted from the expected ToA to shorter/longer ToA, resulting small errors in a ToA estimation caused by the multipath condition.

Figure 11 shows the impulse response of an arbitrary position in channel 9, which gives relatively large minus ranging error. The proposed algorithm cannot find the expected FAP as shown in figure 11. This position is related to far position from the Tx antenna. Figure 12 shows a zoom selection area of impulse response shown in Figure 11. The calculated NF for this point is -104dB, and the FDP level is 14dB higher than this NF, however this peak is not the real FAP, so cause relatively large minus ranging error. Occurrence of this high peak in noise area, cause the wrong first path detection by algorithm, which cannot eliminate even by more accurate NF estimation.

Figure 13 shows the impulse response of an arbitrary positions in channel 9, which gives relatively large positive ranging error. The proposed algorithm cannot find the expected FAP as shown in figure 13. This large error produced because of false estimation of NF by proposed algorithm. In the proposed FAP detection, the detecting of first peak started from SP , going to the origin, and it continue till finding

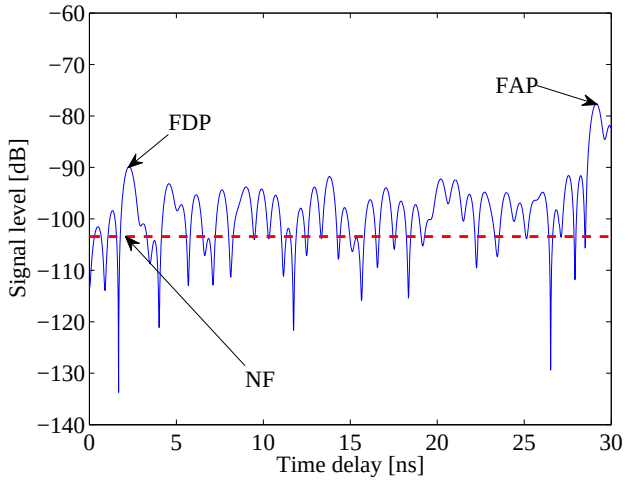

Figure 12 Zoom out of first 30 ns of Figure 11

the first peak higher than calculated NF by L_{th} value. This algorithm has the advantage of detecting the peak after a few iteration number, however for some cases (as shown in Figure 13), the algorithm cannot detect the FAP, and SP detected as FDP. Detection algorithm started from origin and going to SP may eliminate the error of such these cases.

It is observed that the proposed algorithm increase the number of minus errors of the ranging process. This is due to estimating a FDP with a shorter ToA, which in turn can be due to error nous measured data. The improvement of the algorithm is undergoing by investigating the individual impulse responses of the point with a false ranging estimate. First it has to be confirmed if the data for those points are reliable or not.

5. Influence of Frequency Band and Bandwidth

To investigate the influence of frequency band and system bandwidth, evaluation of ranging accuracy were assessed in channel 3, 4, 9 and 11.Figure 14 shows CDF of ranging er-

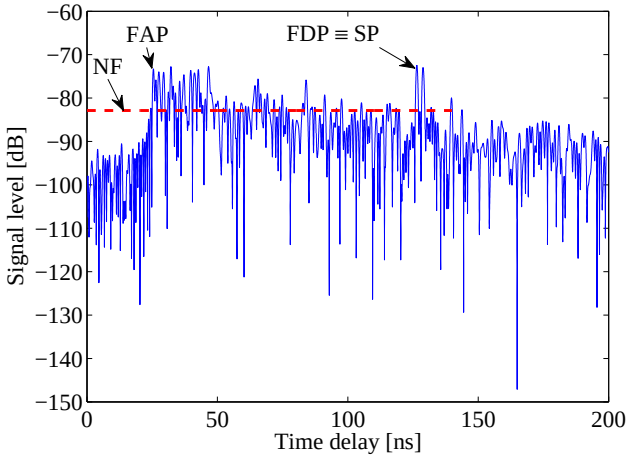

Figure 13 Channel impulse response for an arbitrary position in channel 11

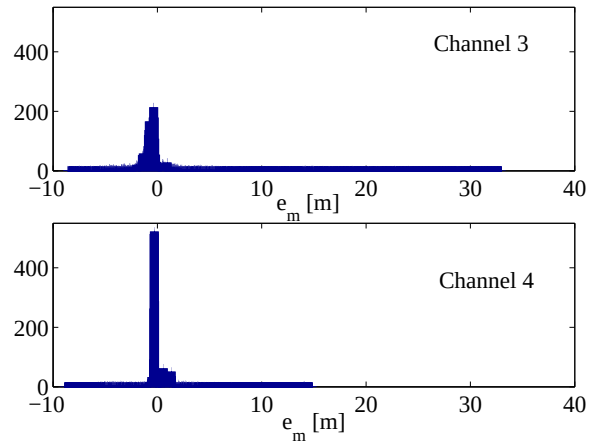

Figure 15 Histogram of ranging error in low sabbands

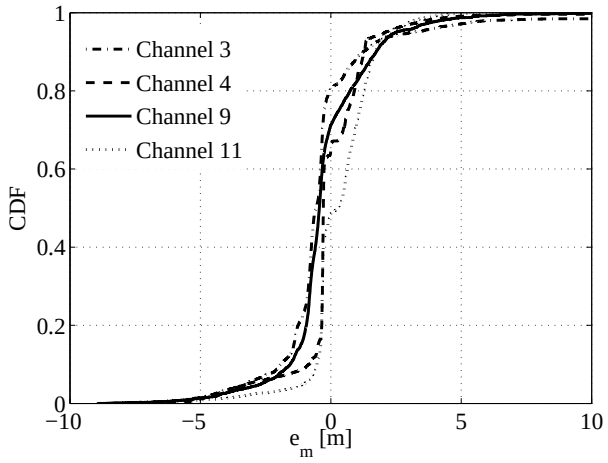

Figure 14 CDF of ranging error in different subbands

ror in these channels obtaining from ToA of FDP. Table 4 shows average and variance of ranging error. Both μ_e and σ_e dramatically decrease in channel 4 compared with channel 3. Figure 15 shows the histogram of ranging error for channels 3 and 4. This figure also shows that by increasing the system band width, the variance of the error decrease. By increasing the system bandwidth ranging accuracy improves. Table 4 also shows that both ranging error average and variance decrease in channel 9 compared with channel 3. Ranging error improves in high bands compared with low bands.

6. Conclusion

An iterative algorithm was proposed for detection of first-arrival path in channel impulse response. Analysis of ranging accuracy based on SP and the first-arrival path was done in this study. This analysis was performed for two allocated mandatory subbands for ranging according to IEEE802.15.4a2007 and two optional subbands. Ranging error was used as an criteria to evaluate the performance of this algorithm. Moreover we study the effect of system bandwidth in the accuracy of indoor localization systems. by increasing the bandwidth the ranging error decrease. The influence of frequency bands on ranging accuracy is also analyzed.

7. Acknowledgement

The authors would like to thank Ms. Huynh Thi Thanh Trieu and Mr. Piao Zhe for their leading initiatives in the measurement and help in data processing.

References

[1] A. Molisch, Ultrawideband propagation channels-theory, measurement, and modeling, IEEE Trans. on Vehic. Technol., Vol. 54, No. 5, 2005,pp. 1528-1545.

[2] Sinan Gezici and zhi Tian, Localization via Ultra-Wideband Radios IEEE Signal Processing magazine, pp. 70-84,July2005.

[3] Yihong Qi and Hisashi Kobayashi, On Time of arrival Positioning in a Multipath Environment IEEE Transaction on vehicular technology,Vol.55,NO.5, pp. 1516-1526,September2006.

[4] M. Ghavami, L. B. Michael, and R. Kohno, Ultra-wideband Signals and Systems in Communication Engineering, Wiley, Hoboken, NJ, 2004.

[5] I. Oppermann, M. Hamalainen, and J. Iinatti, UWB Theory and Applications, Wiley, Hoboken, NJ, 2004.

[6] D. Porcino and W. Hirt, Ultra-wideband radio technology: potential and challenges ahead, IEEE Communications Magazine, Vol. 41, No. 7, July 2003, pp. 66 - 74.

[7] B. Alavi and K. Pahlavan, Bandwidth effect on distance error modeling for indoor geolocation, Proc. IEEE 14th Annual IEEE International Symposium on Personal Indoor and Mobile Radio Communications (PIMRC 2003), Vol. 3, 7-10 Sept. 2003, pp. 2198 2202.

[8] IEEE Std 802.15.4a-2007,pp.81-83.

[9] J.J.Caffery and G.L.Stuber,"Overview of radiolocation in CDMA cellular systems", IEEE Commun. Mag.,Vol.36,no.4,pp.-38-45,Apr.1998.